Temperature evolution of structural and magnetic properties of transition metal clusters

Zacharias Fthenakis[a)]
Institute of Electronic Structure and Laser, FORTH, P.O. Box 1527, 71110 Heraklio, Crete, Greece, and Department of Physics, University of Crete, P.O. Box 2208, 71003 Heraklio, Crete, Greece

Antonis N. Andriotis[b)]
Institute of Electronic Structure and Laser, FORTH, P.O. Box 1527, 71110 Heraklio, Crete, Greece

Madhu Menon[c)]
Department of Physics and Astronomy, University of Kentucky, Lexington, Kentucky 40506-0055, and the Center for Computational Sciences, University of Kentucky, Lexington, Kentucky 40506-0045

(Received 1 August 2003; accepted 26 August 2003)

We report an extension of our tight binding molecular dynamics method [Phys. Rev. B **57**, 10069 (1998)] by incorporating the *Nosé*-bath and the multiple histogram approximations, so as to be applicable to cluster studies at finite temperatures in an efficient way. This generalization allows one to calculate the caloric curve for the cluster and use this to study the effect of temperature on the structural, electronic, and magnetic properties of clusters. The method is used to study the variation of structural and magnetic properties with temperature as well as to obtain the caloric curves of the Ni_{13} cluster. The results are compared with those obtained using classical potentials to describe the interatomic interactions. © *2003 American Institute of Physics.* [DOI: 10.1063/1.1619931]

I. INTRODUCTION

Clusters of transition metal atoms (CTMAs) have attracted major research interest recently, from both a technological and theoretical point of view. However, most of the theoretical investigations have been limited to zero temperature ($T=0$) studies (see Ref. 1 and references therein). All the experimental results reported for these clusters, however, were obtained at $T>0$ and have revealed interesting trends in the evolution of structural, electronic and magnetic properties as a function of their size.[2–8] Even though theoretical calculations performed at zero temperature have had some success in confirming some of the experimental trends, these calculations fail to provide satisfying answers to the structural changes observed in experiments on CTMAs as their size increases.[4,5] These may be attributed to entropic terms missing from $T=0$ considerations.[9,10]

Additionally, study of other *T*-dependent cluster properties also requires the explicit incorporation of temperature effects in theoretical simulations. Such properties include, for example, anomalous evolution with size and temperature of the average magnetic moment per cluster atom ($\langle \mu_i \rangle$) in Fe_n clusters;[7] the experimentally observed lowering of the Curie (T_C) and Debye (Θ_D) temperatures of Co_n clusters as compared to their bulk values;[8] the blocking temperature (T_b) of the clusters; the evolution with size of the various terms that contribute to the specific heat of the cluster;[7,11] the temperature-induced phase transition (especially the second-order phase transition, i.e., from ferromagnetic to paramagnetic state);[7] the thermal expansion coefficient of the cluster,[12] etc. The theoretical study of these properties poses a severe challenge to computational schemes limited to $T=0$. For this reason, dynamical properties of clusters have been mostly studied using simple classical potentials neglecting the detailed electronic structure of the cluster.

It should be noted that the structural properties of transition metal clusters are intricately linked to the magnetic properties, and *vice versa*. Any realistic simulations of structural properties of CTMAs at finite temperatures must, therefore, also incorporate a dynamic consideration of magnetic effects. To the best of our knowledge, theoretical simulation methods incorporating both structural and magnetic effects at finite temperatures have not been used in the case of CTMAs until the present.

In the present work, we extend our zero-temperature tight-binding molecular dynamics (TBMD) method[1] to include the nonzero temperature regimes using the multiple histogram method (MHM)[13,14] and the *Nosé–Hoover* thermostat method.[13–20] We, thus, retain the quantum mechanical approach in which a full description of the electronic structure of the cluster is accounted for within the tight-binding (TB) approximation. Entropic terms of free energy are explicitly included in our method by construction, as discussed below. The present generalization allows us to construct the caloric curve of the system and then use it to calculate the thermodynamic properties of the cluster. Briefly, the basic features of our method are as follows.

II. BRIEF REVIEW OF COMPUTATIONAL METHOD

At $T>0$ a transition metal cluster, when thermalized in a heat bath, is described by the canonical probability distribution function of total energy, $P_T(E)$, which specifies the probability that the system will be found in the energy inter-

a)Electronic mail: fthenak@iesl.forth.gr
b)Electronic mail: andriot@iesl.forth.gr
c)Electronic mail: super250@pop.uky.edu

val $[E,E+\Delta E]$ at the specified temperature T. The distribution function corresponding to this temperature, within the canonical ensemble description, is[13,14,17–20]

$$P_T(E)=\frac{n_T(E)}{N_T}=\frac{[\Delta\Gamma(E)]e^{-E/k_BT}}{Z_T}, \tag{1}$$

where $n_T(E)$ is the number of states in the energy interval $[E,E+\Delta E]$, N_T is the total number of accessible states, k_B is Boltzmann's constant, $\Delta\Gamma(E)$ is the number of all the different states with energy in the interval $[E,E+\Delta E]$ and Z_T the partition function at temperature T,

$$Z_T=\sum_i \exp(-\beta E_i)=\sum_{E_i} \Delta\Gamma(E_i)\exp(-\beta E_i). \tag{2}$$

A molecular dynamics (MD) simulation at a given temperature T provides numerical values for $n_T(E)$ at every accessible energy E. Let these energies lie in the interval $[E_{\min},E_{\max}]$. We discretize this energy interval (in N intervals, each of width ΔE) for a given set of temperatures T_j, $j=1,...,M$. We then take the logarithm of both sides of Eq. (1) in the discretized version and define the quantity R_{ij} in the form of a finite set of algebraic equations, as follows:

$$R_{ij}=\ln\frac{n_{T_j}}{N_{T_j}}+\frac{E_i}{k_BT_j}-\ln[\Delta\Gamma(E_i)]+\ln Z_{T_j},$$
$$i=1,...,N; \quad j=1,...,M. \tag{3}$$

Note that in the exact case, $R_{ij}=0$. The system of Eqs. (3) is overdetermined, as it includes $N+M$ unknowns [i.e., the terms $\Delta\Gamma(E_i)$ and Z_{T_j}] in terms of $N\times M$ equations. For such a system, the determination of the unknown terms can be achieved by employing a nonlinear least square fitting. In particular, we make use of the proposed MHM.[13,14,17–20] According to this method, the maximum likelihood estimator χ^2 is defined as

$$\chi^2=\sum_{i=1}^{N}\sum_{j=1}^{M} n_{T_j}(E_i)R_{ij}^2, \tag{4}$$

subject to the requirements

$$\frac{\partial\chi^2}{\partial\ln[\Delta\Gamma(E_i)]}=0, \quad i=1,...,N;$$
$$\frac{\partial\chi^2}{\partial\ln Z_{T_j}}=0, \quad j=1,...,M. \tag{5}$$

This procedure sets up $N+M$ equations in $N+M$ unknowns. The solution of the system of Eqs. (5) becomes feasible in two steps. In the first, the partition functions Z_{T_j} for a finite set of temperatures T_j, $j=1,...,M$ ($M\approx200$) are obtained. In the second step, we compute the entropy terms $S(E_i)=k_B\ln[\Delta\Gamma(E_i)]$ (within an additive constant) for a much larger set of energy values E_i, $i=1,...,N$ ($N\approx6000$).[17]

We next generalize our TBMD scheme for transition metal systems used previously in the $T=0$ case[1] by incorporating the *Nosé–Hoover* thermostat method,[13–18] which is a constant temperature method in an extended system scheme that includes an extra degree of freedom, ζ, which ensures that the system is in thermodynamic equilibrium with a heat bath. As a result, the equations of motion for a cluster consisting of N_{cl} atoms in contact with a heat bath at temperature T can be generalized as follows:

$$\frac{d\mathbf{p}_i}{dt}=-\frac{\partial E}{\partial\mathbf{r}_i}-\zeta\mathbf{p}_i, \quad i=1,...,N_{cl}, \tag{6}$$

$$\frac{d\zeta}{dt}=\frac{2}{W}\left\{\sum_{i=1}^{N_{cl}}\frac{p_i^2}{2m_i}-\frac{f}{2}k_BT\right\}, \tag{7}$$

where E is the total energy of the cluster obtained using the TBMD method, W is a parameter representing the *mass* of the heat bath, and f is the number of degrees of freedom for the system (i.e., $f=3\,N_{cl}$-6 for a cluster with no rotational or translational degrees of freedom).

The details of our tight-binding molecular dynamics (TBMD) scheme can be found in Ref. 1. Here we give a brief overview.

The total energy E is written in its general form as a sum of several terms,[1]

$$E=U_{el}+U_{rep}+U_0, \tag{8}$$

where U_{el} is the sum of the one-electron energies E_n for the occupied states:

$$U_{el}=\sum_n^{occ} E_n. \tag{9}$$

In the tight-binding scheme E_n is obtained by solving the characteristic equation:

$$(\mathbf{H}-E_n\mathbf{1})\mathbf{C}^n=0, \tag{10}$$

where $\mathbf{H}$ is the Hamiltonian of the system.

The Hellmann–Feynman theorem for obtaining the electronic part of the force is given by[1]

$$\frac{\partial E_n}{\partial x}=\mathbf{C}^{n\dagger}\frac{\partial\mathbf{H}}{\partial x}\mathbf{C}^n. \tag{11}$$

Our TBMD scheme for a single-species system is based on a minimal set of five adjustable parameters. These parameters are determined by fitting to experimental data for quantities such as the bond length, the vibrational frequency, and the binding energy of the dimer, the cohesive energy of the corresponding bulk state, and the energy level spacing of the lowest magnetic states of the dimer and trimer clusters. In the absence of experimental data, we fit to data for small clusters obtained using *ab initio* methods. The fixed set of TB parameters are obtained from the universal scheme proposed by Harrison[22] suitably scaled with respect to the interatomic distance.[1]

For discussion purposes (see below) we recall that the Slater–Koster tight-binding parameters, $V_{kl\mu}(r)$, have the following dependence on the interatomic distance r in the original TBMD scheme:[21]

$$V_{kl\mu}(r)=V_{kl\mu}^{(0)}(r)\,\theta(R_{cutoff}-r),$$
$$k,l=s,p,d,...; \quad \mu=\sigma,\pi,\delta,..., \tag{12}$$

where the matrix elements $V_{kl\mu}^{(0)}(r)$ are given in terms of the universal matrix elements of Harrison,[22] $\theta(x)$ is the step function, and R_{cutoff} is a cutoff distance beyond which the interatomic interaction is taken to be zero.

The total energy expression also derives contributions from ion–ion repulsion interactions. This is approximated by a sum of pairwise repulsive terms and included in U_{rep}. This sum also contains the corrections arising from the double counting of electron–electron interactions in U_{el}.[1] At zero temperature, the U_0 is a constant that merely shifts the zero of energy; it is expressed as a function of the number of the interatomic bonds developed in the cluster.[1]

It is apparent that at zero temperature there is no contribution of the U_0 term to the total force. The contribution from U_{rep}, on the other hand, is rather straightforward. One can then easily do molecular dynamics simulations by numerically solving Newton's equation,

$$m\frac{d^2x}{dt^2}=F_x=-\frac{\partial E}{\partial x}, \tag{13}$$

to obtain x as a function of time.

At nonzero (and especially large) temperatures, the U_0 term can contribute to the total force per atom, since the bond lengths (and consequently the number of bonds) are allowed to vary in a larger range than in the case of $T=0$. The effect of bond length variation will be minimal if the variation is such that the bonds remain within the cutoff distance R_{cutoff}.

III. RESULTS AND DISCUSSION

We choose the Ni_{13} cluster as a prototype for the application of our formalism since this system has been previously studied for structural properties at finite temperatures, although using only classical interatomic potentials and without the consideration of any magnetic effects.[23–25]

By performing a series of MD simulations (of approximately 2×10^6 time steps each) we obtain the probability distribution function, $P_T(E)$ [Eq. (1)], for temperatures ranging from 0 to 700 K. These distributions contain the full thermodynamic information (for this temperature range), as they allow us to derive the caloric curve (CC) of Ni_{13}. Within the MHM, we solve Eqs. (5) and obtain the number of states $\Delta\Gamma(E_i)$. From these, the partition function, Z_T, can be obtained [according to Eq. (2)] from which we calculate the total energy. The efficiency of the MHM is that it can be applied using a relatively small number of distributions $P_T(E)$, provided that they exhibit considerable overlap among themselves. It should be noted that the microcanonical CC can be obtained by plotting the energies of the extrema of $P_T(E)$ versus the temperature,[11] while the canonical CC can be obtained simply by plotting $\langle E(T)\rangle = \int E P_T(E)dE$ versus temperature.

In Fig. 1 we present two independent calculations of the average total energy per atom, $\langle E(T)\rangle/N_{\text{cl}}$, as a function of temperature. The solid curve corresponds to the result obtained from the equation $\langle E(T)\rangle=-\partial \ln Z_T/\partial\beta$, $\beta=1/k_{\text{B}}T$, i.e., the outcome of the MHM. The dashed curve corresponds to the time average energy, $\langle E(T)\rangle$, obtained from the tight-binding total energy expression given by Eq. (8). In the inset we present the entropy function, S, as a function of the energy per atom ($S=k_{\text{B}}\ln\Delta\Gamma$). The accuracy of the MHM-derived energy curve is limited at very low temperatures because of the very small overlap of the distribution functions $P_T(E)$ (which behave as δ functions at these temperatures). Similarly, the accuracy is also limited at the high-temperature end as in this region information is needed from distributions at higher temperatures. In both cases, however, the accuracy can be improved according to the requirements of the solution either by taking distributions at a finer temperature mesh at low temperatures or including distributions for higher temperatures.

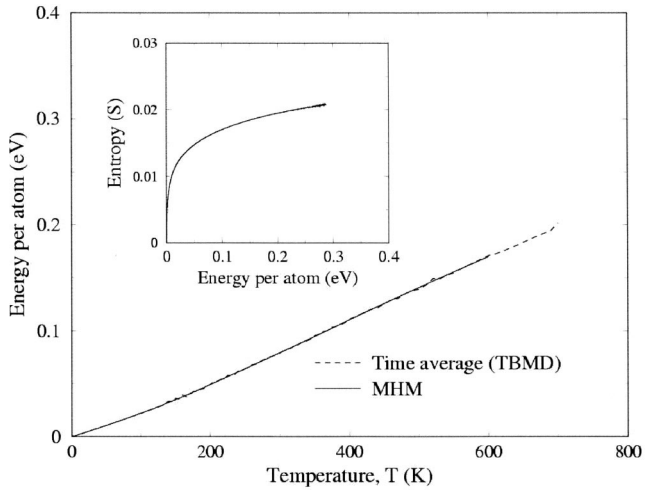

FIG. 1. Two independent calculations of the average total energy per atom, $\langle E(T)\rangle/N_{\text{cl}}$, as a function of temperature. The solid curve corresponds to the result obtained from the equation $\langle E(T)\rangle=-\partial \ln Z_T/\partial\beta$, $\beta=1/k_{\text{B}}T$, i.e., the MHM. The dashed curve corresponds to the time-averaged total energy per atom obtained from the tight-binding total energy expression. In the inset we present the entropy function as a function of the energy per atom.

In Fig. 2 we present the results for the heat capacity

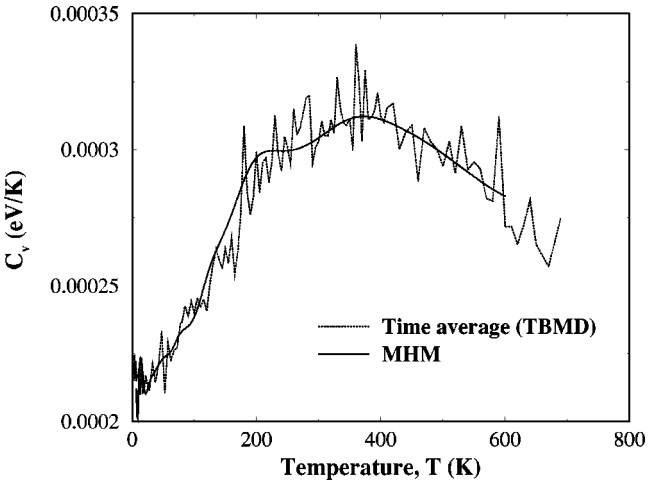

FIG. 2. Two independent calculations of the specific heat per atom, c_V, of Ni_{13} as a function of temperature. The solid curve is obtained from the slope of the solid curve of Fig. 1. The dashed curve is obtained from the equation $c_V=(1/N_{\text{cl}}k_{\text{B}}T^2)(\langle E^2\rangle-\langle E\rangle^2)$, where $\langle E^2\rangle$ and $\langle E\rangle$ are time averages obtained according to the TB total energy expression (see the text).

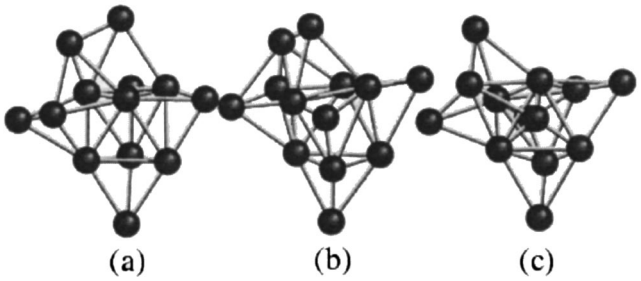

FIG. 3. Snapshots of the ground state geometry of Ni_{13} at (a) 0, (b) 100, and (c) 200 K.

$c_V(T)/N_{\mathrm{cl}}$ as a function of the temperature using two independent approaches. In particular, the solid curve refers to the result obtained according to the formula $c_V(T) = \partial\langle E(T)\rangle/\partial T$ (i.e., from the slope of the solid curve of Fig. 1 that is the result of the MHM). The dotted curve for c_V is obtained from the following equation: $c_V=[1/k_{\mathrm{B}}T^2)(\langle E^2\rangle - \langle E\rangle^2)]$, where both $\langle E^2\rangle$ and $\langle E\rangle^2$ are time-averaged values obtained directly from the MD simulations and are obtained from the tight-binding total energy expression [i.e., that of Eq. (8).[1] Once again, it is clear from this figure that the MHM leads to more smooth results due to its efficiency in providing data for an infinitely dense mesh of temperature points. However, the accuracy of the results is very poor for $T<50$ K for reasons explained in the previous paragraph.

It is apparent from Figs. 1 and 2 that our results using the two methods for the Ni_{13} cluster are very similar and, therefore, appear to be independent of the numerical procedure that is used and validates the accuracy and applicability of the method we propose. In particular, we find that Ni_{13} is very stable (retaining its zero-temperature geometry, i.e., that of a distorted prismlike structure[1]) up to the transition temperature $T_{\mathrm{trans}}\approx 180$ K, beyond which it undergoes a phase transition. In Fig. 3 we present snapshots of the Ni_{13} cluster prior and after the phase transition (i.e., at temperatures 0, 100, and 200 K, respectively). We find that for $T<T_{\mathrm{trans}}$ the cluster geometry exhibits a resonance structure that is a mixture of two isoenergetic mirror geometries. For $T>T_{\mathrm{trans}}$ the cluster departs from these two geometries, with its shape changing as the temperature increases.

The phase transition is indicated by a change in the slope of the caloric curves shown in Fig. 1. We note that simulations using classical potentials predict a transition temperature for this cluster, ranging from 240–1700 K, depending strongly on the type of the classical potential used (see below).[23–25]

In our case, the existence of a phase transition at 180 K is more clearly shown in Fig. 4, where we present the Lindemann index (or the root mean square bond length fluctuation)[27,28] for the Ni_{13} cluster. In Fig. 4, we present the Lindemann index, δ, as a function of temperature obtained from the formula

$$\delta=\frac{2}{N_{\mathrm{cl}}(N_{\mathrm{cl}}-1)}\sum_{i=1}^{N_{\mathrm{cl}}}\sum_{j>i}^{N_{\mathrm{cl}}}\frac{\sqrt{\langle r_{ij}^2\rangle-\langle r_{ij}\rangle^2}}{\langle r_{ij}\rangle}. \tag{14}$$

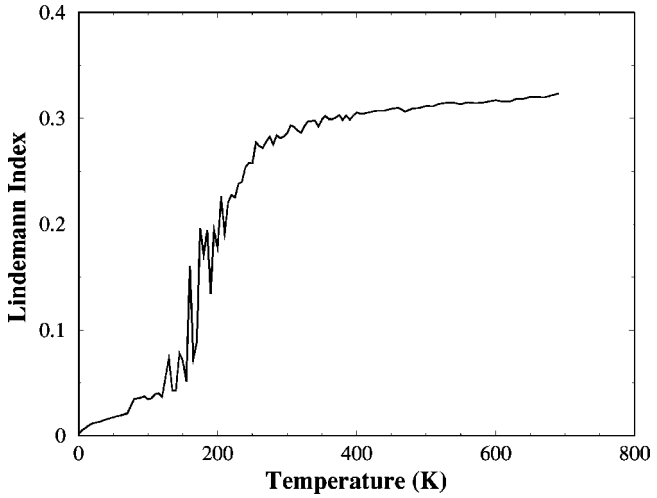

FIG. 4. The Lindemann index of Ni_{13} as a function of temperature.

The Lindemann index is associated with the phase transition from a solid to a liquid. As Fig. 4 shows, there is a phase transition (for $\delta>0.1$) near 180 K.

In order to investigate the large discepancy in the transition temperature found between our results and those reported in Ref. 23, we performed the following two tests. In the first, we applied the MHM [described by Eqs. (1)–(7)] using the classical potential, as used in Ref. 23. This simulation reproduced exactly the results of Ref. 23 for the geometry (icosahedral) and the T_{trans}. We note, however, that the classical potential employed in Ref. 23 fails to reproduce known results for small clusters as, for example, the bond length and vibrational frequency of the Ni_2 dimer.[29] In our second test we first modified the classical potential so as to reproduce the experimentally known small cluster data and repeated the calculations to determine the transition temperature. This modified classical potential produced a transition temperature much lower in value than the 800 K in Ref. 23. In particular, we found a transition temperature of $\approx$320 K. A lower transition temperature $T_{\mathrm{trans}}=280$ K was also obtained using the potential proposed by Uppenbrink and Wales.[25] This potential combines the two-body Lennard-Jones terms with three-body Axilrod–Teller terms and was claimed suitable for cluster calculations. It is worth noting that this potential predicts a ground state geometry for Ni_{13} that exhibits a C_{2v} symmetry, in close agreement with the results of our TBMD method.[1]

The tests described above suggest the source of a possible error that is inherent in the construction of the classical interatomic potential that is used. Furthermore, the results of our second test allow us to claim that both the TB and the classical description of the interatomic potential could lead to equivalent results if this error is properly corrected. According to our findings, such corrections should be applied in the case of the classical approach in fitting the classical interatomic potentials so as to reproduce small cluster properties in agreement with known experimental results.

In addition to the above conclusions, the present results have indicated that the MHM is very efficient when used in combination with a classical interatomic potential, provided

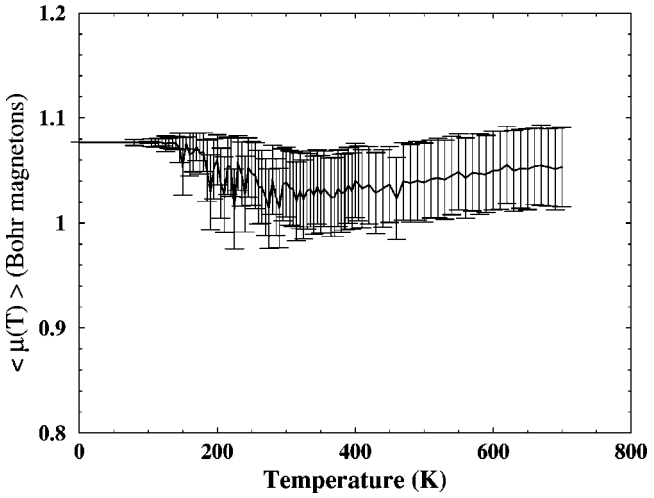

FIG. 5. The average magnetic moment ($\langle \mu(T) \rangle$) (per cluster atom) for the Ni_{13} cluster as a function of temperature using the present method. Error bars are indicated by the short straight vertical lines.

the latter accurately describes the small cluster results. This is a significant conclusion since for systems consisting of very large number of atoms one needs to use classical potentials as the TBMD method becomes computationally prohibitive.

In agreement with Ref. 23, we find that the calculated specific heat c_V of Ni_{13} (see Fig. 2) exhibits a resonancelike peak at the transition temperature. It is also worth pointing out that in Ref. 23, constant-energy (microcanonical ensemble) simulations were performed, while in the present work we use the constant-temperature (canonical ensemble) simulations. Classical potentials have also been used to study the Ni_{429} cluster with the transition temperature predicted to be 1400 K.[26]

Finally, we present our results for the magnetic moment, $\mu(T)$, of the Ni_{13} cluster using our method. In Fig. 5, we show the temperature dependence of $\mu(T)$ for T up to 700 K. For each temperature, the magnetic moment shown in Fig. 5 is the statistical time average of the magnetic moment per cluster atom. The standard deviation is found to be a function of temperature; it is nearly zero for temperatures less than 100 K and gets larger as the temperature increases, reaching its maximum value ($\approx \pm 5\%$) for $T > T_{\text{trans}}$. As seen in the figure, the magnetic moment does not change appreciably with temperature, remaining within the range specified by the calculated error bars. It is worth noting that for $T > T_{\text{trans}}$, the magnetic moment starts decreasing, slightly reaching a minimum ($\approx 5\%$ lower than its zero temperature value) and stays at this value (with a tendency to increase slightly) at greater temperatures. As these changes of the average value of the magnetic moment per cluster atom are well within the error bars, one cannot claim with any certainty how the magnetic moment changes with temperature. The most significant results emerging from the present calculations, however, is the width of the expected distribution of the $\mu(T)$ values. This indicates that even within the approximation of a single domain particle (i.e., with all magnetic moments of cluster atoms aligned collinearly) the magnetic moment of the cluster exhibits significant error bars, even at low enough temperatures. Nevertheless, the temperature-induced changes in the magnetic moment of the cluster are not as dramatic as the corresponding structural changes of the cluster. This is significant observation because it suggests that the determination of the magnetic moment of the cluster does not require the accuracy needed in specifying the temperature-induced structural phase transitions.

The temperature dependence of $\mu(T)$ found in the present calculations is attributed to the existence of many isomers of Ni_{13}, which are the result of changes in the interatomic distances and the charge transfers that take place in the cluster as the temperature is varied. The temperature-induced changes in the interatomic distances result in local changes of the atom-coordination number and also in appreciable changes in the charge transfer among the cluster atoms with a corresponding redistribution of spin-up and spin-down electrons. The $\mu(T)$ dependence, thus, is different in origin from that found if it is assumed that the single particle is not a strictly single domain particle as, for example, in the study of Vargas *et al.*[30] Nevertheless, the present approach can be easily generalized to the study of magnetic properties of clusters that exhibit atoms with noncollinear magnetic moments as well.

IV. CONCLUSION

We have presented an efficient generalization of our zero-temperature TBMD method, which enables a quantum mechanical approach for studying structural, electronic, and magnetic properties of transition metal clusters as a function of temperature and a canonical ensemble statistics. An application of the method to the Ni_{13} cluster shows significant differences from works reported using classical potentials and microcanonical ensemble statistics. We have shown that these differences may be attributed to the inadequecy of the existing classical potentials to describe the known properties of small Ni clusters. We have also shown that when this factor is accounted for properly, the two methods can give results in good agreement with each other. The incorporation of the temperature shows interesting variations of many physical properties as a function of temperature as, for example, structural and magnetic phase changes. Of particular interest in the present work appears to be the results for the magnetic moment of the Ni_{13} cluster as a function of temperature that indicate relatively large deviations of the average value of the magnetic moment. These were attributed to the existence of various isomers of Ni_{13} that can be reached by thermal activation.

ACKNOWLEDGMENTS

The present work is supported through grants by EU-GROWTH research project AM-MARE (G5RD-CT-2001-00478), the National Science Foundation (NSF) (ITR-0221916), Department of Energy (DOE) (00-63857), NASA (00-463937), and the Kentucky Science & Technology Corporation (03-60214).

[1] A. N. Andriotis and M. Menon, Phys. Rev. B **57**, 10069 (1998).
[2] I. M. L. Billas, A. Chatelain, and W. A. de Heer, Science **265**, 1682 (1994).

[3] S. E. Apsel, J. W. Emmert, J. Deng, and L. A. Bloomfield, Phys. Rev. Lett. **76**, 1441 (1996).
[4] E. K. Parks, K. P. Kerns, and S. J. Riley, J. Chem. Phys. **109**, 10207 (1998); **114**, 2228 (2001).
[5] E. K. Parks, G. C. Nieman, K. P. Kerns, and S. J. Riley, J. Chem. Phys. **108**, 3731 (1998).
[6] M. Schmidt, R. Kusche, W. Kronmuller, B. von Issendorff, and H. Haberland, Phys. Rev. Lett. **79**, 99 (1997).
[7] D. Gerion, A. Hirt, I. M. L. Billas, A. Chatelain, and W. A. de Heer, Phys. Rev. B **62**, 7491 (2000).
[8] M. Hou, M. E. Azzaouri, H. Pattyn, J. Verheyden, G. Koops, and G. Zhang, Phys. Rev. B **62**, 5117 (2000).
[9] J. P. K. Doye and D. J. Wales, Phys. Rev. Lett. **80**, 1357 (1998).
[10] J. P. K. Doye and F. Calvo, Phys. Rev. Lett. **86**, 3570 (2001).
[11] M. Schmidt, R. Kusche, T. Hippler, J. Donges, W. Kronmuller, B. von Issendorff, and H. Haberland, Phys. Rev. Lett. **86**, 1191 (2001).
[12] S. Kummel, J. Akola, and M. Manninen, Phys. Rev. Lett. **84**, 3827 (2000).
[13] P. Labastie and R. L. Whetten, Phys. Rev. Lett. **65**, 1567 (1990).
[14] A. M. Ferrenberg and R. H. Swendsen, Phys. Rev. Lett. **61**, 2635 (1998).
[15] S. Nosé, Mol. Phys. **52**, 255 (1984); J. Chem. Phys. **81**, 511 (1984).
[16] W. G. Hoover, Phys. Rev. A **31**, 1965 (1985).
[17] S. Weerasinghe and F. G. Amar, J. Chem. Phys. **98**, 4967 (1993).
[18] R. Poteau, F. Spiegelmann, and P. Labastie, Z. Phys. D: At., Mol. Clusters **30**, 57 (1994).
[19] D. J. Evans and B. L. Holian, J. Chem. Phys. **83**, 4069 (1985).
[20] G. S. Fanourgakis, S. C. Farantos, P. Parneix, and Ph. Brechignac, J. Chem. Phys. **106**, 4954 (1997).
[21] J. C. Slater and G. F. Koster, Phys. Rev. **94**, 1498 (1954).
[22] W. Harrison, in *Electronic Structure and Properties of Solids* (Freeman, San Francisco, 1980).
[23] S. K. Nayak, S. N. Khanna, B. K. Rao, and P. Jena, J. Phys.: Condens. Matter **10**, 10853 (1998).
[24] Y. J. Lee, J. Y. Maeng, E.-K. Lee, B. Kim, S. Kim, and K.-K. Han, J. Comput. Chem. **21**, 380 (2000).
[25] J. Uppenbrink and D. J. Wales, J. Chem. Phys. **96**, 8520 (1992).
[26] B. Gunes and S. Erkoc, Int. J. Mod. Phys. C **11**, 1567 (2000).
[27] J. J. Gilvarry, Phys. Rev. **102**, 308 (1956).
[28] D. D. Frantz, J. Chem. Phys. **102**, 3747 (1995).
[29] The use of the classical potential of Ref. 23 leads to the following results for the Ni_2 dimer bond length 2.04 Å and vibration frequency 502 cm^{-1} [to be compared to the experimental values 2.20 Å and 330 cm^{-1}, respectively (Ref. 1)].
[30] P. Vargas, J. d' Albuquerque e Castro, and D. Altbir, Phys. Rev. B **60**, 6541 (1999).